Journal of Network and Computer Applications 52 (2015) 69–78

Contents lists available at ScienceDirect

Journal of Network and Computer Applications

journal homepage: www.elsevier.com/locate/jnca

Effective link interference model in topology control of wireless Ad hoc and sensor networks

Guodong Sun [a,*], Lin Zhao [a], Zhibo Chen [a], Guofu Qiao [b]

[a] School of Information Science and Technology, Beijing Forestry University, Beijing 100083, China
[b] School of Civil Engineering, Harbin Institute of Technology, Harbin 150006, China

ARTICLE INFO

Article history:
Received 25 August 2014
Received in revised form
21 November 2014
Accepted 31 January 2015
Available online 16 March 2015

Keywords:
Wireless sensor networks
Link interference model
Topology control
Energy spanner

ABSTRACT

Topology control is an important way of reducing the link interference in wireless Ad hoc and sensor networks with shared channel. Modeling link interference is the primary step for designing interference-aware topology controls, and it is very critical to the efficacy of the topology control schemes in use. This paper presents a new link interference model, which can not only be easily calculated with global or local algorithms, but also more effectively profile the link interference in co-channel wireless Ad hoc and sensor networks than previous models. Based on the proposed model, a centralized topology control algorithm is designed to construct interference-optimal topologies. In fact, our model can also be fed into most of the already-existed topology control algorithms aimed at reducing link interferences. Finally, extensive simulations and analysis are conducted to evaluate our designs in detail. The simulation results show the outstanding effectiveness of interference reduction achieved by our model and algorithm, in comparison with the previous work.

1. Introduction

Wireless Ad hoc and sensor networks (Yick et al., 2008; Chong and Kumar, 2003; Schmid and Wattenhofer, 2006; Ababneh, 2010; Liu et al., 2012) are so constrained in energy, bandwidth, and computation that the energy efficiency and the network capacity are rather hard to be achieved. Recently, topology controls (Aziz et al., 2013) are recognized as an effective way that can reduce energy consumption and improve the network throughput while guaranteeing necessary network properties, such as network connectivity and path spanner. For wireless Ad hoc and sensor networks, especially large-scale ones, almost all nodes share a low-rate and low-power radio spectrum (for instance, the widely used IEEE 802.15.4 is of rate 250 kbps at mW level)—a great many concurrent co-channel communications possibly pervade throughout the whole network, which will degrade the network performances severely. Hence, the control and reduction of interferences caused by co-channel communications is a very important topic in designing effective and efficient topology control policies for wireless Ad hoc and sensor network (Jain et al., 2003; Enam et al., 2014; Lee and Yang, 2012).

Recently, some topology control algorithms (Burkhart et al., 2004; Johanasson and Carr-Motyckova, 2005; Moaveni-Nejad and Li, 2005; Moscibroda et al., 2006; Blough et al., 2007; Chiwewe and Hancke, 2012) have been proposed for wireless Ad hoc and sensor networks, to deal with the co-channel link interferences. In the first place, the key step facing interference-aware topology control algorithms is that of choosing which model to measure the interference of link or node. Most of the existed works use the nodes-covered-based model, which measures the interference caused by a link according to the number of nodes this link covers. Such a model is, however, either too strict to be implemented in practice, or ineffective to reflect the real situation of link interferences, and then incapable of achieving sufficiently interference-aware topologies while assuring other important network properties.

To address such a problem, this paper first identifies the limitations of previous link interference models in reality, and then presents a simple-but-effective model which measures the interference of a given link only by counting the number of links that are actually interfered with this given link. Also, a centralized algorithm and extensive simulations are designed and implemented, to evaluate the proposed link interference model. Especially the proposed algorithm can achieve provable interference-optimal topology of energy spanner. Simulation results show that our designs dramatically reduce the number of links left in the constructed topologies, and consequently achieve lower network interference than previous approaches, while guaranteeing the network connectivity and the energy spanner properties.

The rest of this paper is organized as follows. Section 2 overviews the major early works related to ours. Section 3 introduces some assumptions used in this paper, presents a new interference model for wireless Ad hoc and sensor networks, and finally proposes a centralized algorithm that can generate an interference-optimal topology

* Corresponding author.
E-mail address: sungd@bjfu.edu.cn (G. Sun).

http://dx.doi.org/10.1016/j.jnca.2015.01.006
1084-8045/

of energy spanner. Section 4 presents and deeply analyzes the simulation results. Section 5 concludes this study.

2. Related work

To quantify the link-level interference in wireless Ad hoc and sensor networks, there are roughly three kinds of models proposed in the literature: the link-level, the node-level, and the path-level models. We next review these three models and the topology control optimizations based on these models. And we will discuss the shortcomings facing these models later in Sections 3.1 and 3.2.

Burkhart et al. (2004) (and later in Rickenbach et al., 2005, 2009) propose a link interference model that measures the interference of a link by the number of nodes this link can cover. It works like this (1) given a link $\ell_{u,v}$ connecting nodes u and v, there are two node sets, V_u and V_v such that all nodes in V_u and V_v are covered by u and v, respectively; and (2) $|V_u \cup V_v|$ serves as the measure of the interference (also called the coverage) of link $\ell_{u,v}$. The authors (Burkhart et al., 2004) assumed that the coverage of wireless node is a disk and that the transmit power of node can be adjusted to any level within zero and the maximum radio range. Centralized and local algorithms are designed in Burkhart et al. (2004) to achieve interference-optimal topologies. But authors (Moaveni-Nejad and Li, 2005) argue that in reality, wireless nodes cannot adjust their transmit power at will and then they modify Burkhart's model: they propose a model which measures the interference of a link by the number of links incident with this link. Additionally (Moaveni-Nejad and Li, 2005) also involves a node-level interference model which defines the interference of a node as the number of nodes locating within its transmit range. Macedo et al. (2009) design a TDMA-based MAC scheme for wireless sensor networks that is based on the interference actually experienced by nodes.

Unlike the two above models (Burkhart et al., 2004; Moaveni-Nejad and Li, 2005) in which each node covers a disk area, Blough et al. (2007) employ more realistic energy models taking into account the shadowing and fading effects, to determine the interference range of a link. Their link interference is measured by the interference number which is calculated based on the real coverage region derived by the transmit power of link. In essence, like models in Burkhart et al. (2004) and Moaveni-Nejad and Li (2005), the model in Blough et al. (2007) is still based on the number of nodes that a link can cover, while the difference merely resides in how to determine whether a node is covered (interfered with) by another node. We call such models the nodes-covered-based interference model.

A path-level interference metric is proposed by Johanasson and Carr-Motyckova (2005), who consider the length of the paths in network graph; but calculating the path metric still depends on the interferences of links along the path. Blough et al. (2007) take into account the multi-hop interference which is, however, also measured by the sum of the interferences of all links along the path. Based on the specified interference models, these previous works propose algorithms with different objectives and network property guarantees. Network connectivity and spanner are two major properties that the topology control algorithm should assure. To optimize the network-level interference, usually, the maximum link (or node) interference and the average of link (or node) interference are treated to be the optimization objectives. For existing approaches, the greedy policy is often used to achieve interference-optimal topology, either in a centralized manner or in a distributed manner. Chiwewe and Hancke (2012) propose a distributed interference-reducing scheme which constructs connected topology based on Yao and Gabriel graphs rather than on the optimization under any interference model described in advance.

There have been another kind of works focusing on measuring link interference in wireless sensor networks. Liu et al. (2010) present a passive interference measurement approach to deriving the actual physical interference. Huang et al. (2011) present an accuracy-aware method of modeling and measuring link interference. SoNIC (Hermans et al., 2013) is proposed to detect interference among 802.15.4 sensor networks sharing 2.4 GHz with other Bluetooth and WiFi devices. These works mentioned above are aimed at estimating local link interferences by empirically measuring *in situ* link quality in terms of RSSI, LQI, SINR, or PRR, without considering how to reduce global link interferences from the angle of topology controls.

3. Designs

In this section, we first introduce some realistic network models and assumption used in this paper; second, we present a simple-but-effective interference model and its motivation; third, we propose a centralized algorithm to optimize the interference all over the network. Finally, some comprehensive design considerations are provided.

3.1. Network model and assumptions

Wireless Ad hoc and sensor networks are often consisted of a lot of wireless nodes, which are placed in some area to form a flexible communication infrastructure, or to monitor physical events, like the light strength, the temperature and so on. We assume that all nodes in the wireless Ad hoc or sensor networks will keep stationary once they are deployed. We use the graph notation, $G(V,E)$ to describe the network connection: all nodes form the node set V and all possible links the edge (link) set E.

We assume two-way links—there exists a link between two nodes if and only if both of them can correctly receive data sent out by each other. For two communicating nodes, in reality, an ACK message sent by the receiver is usually used to indicate a correct reception of packet; like the data transmission, the ACK message will also consume the bandwidth and energy. Hence, the assumption of two-way link is more realistic than the UDG (unit-disk graph) model, which is adopted by most previous approaches. The network graph derived by the two-way links is obviously undirected. We also assume that each node can adjust its transmission power, continually or discretely, within a given range. For example, the CC1000 and CC2420 radio chips, equipped in Mica sensor mote and Telosb sensor mote, respectively, both have a few transmit power levels that can be dynamically configured by programs. It is assumed that two communicating nodes always use the lowest possible transmit power to reach to each other. It is worthy to note that we neither assume the homogeneous transmit power of node all over the network, nor require that a sender and its receiver have to use the same transmit power.

For a pair of nodes, u and v in a given network, $G(V,E)$, if both of them can communicate directly, we then assume that the energy budget for carrying out one two-way communication over link $\ell_{u,v}$ is proportional to the square of the Euclidean (physical) distance from u to v. For the simplicity, we use $|uv|$ and $\|uv\|$ to represent the physical distance of link $\ell_{u,v}$ and the energy needed by the communication over $\ell_{u,v}$, respectively.

3.2. The interference model

Before describing our interference model, we first give some notations. If the Euclidean distance from node x to node u is d and d is less than or equal to the maximum radio range of u, we say that x is d-covered by u, or u d-covers x. That one node d-covers another

node, however, does not hold visa versa. Similarly, we say that x is d-covered by link $\ell_{u,v}$ if x is d-covered by at least one of u and v.

The previous works measure the interference of a given link according to the number of nodes the link can cover. Such a way of calculating link interference is, however, possibly inapt or even futile sometimes.

First, for Topo-I shown in Fig. 1, the $\ell_{u,v}$ link $|uv|$-covers nodes a, b, and c, and then the interference of $\ell_{u,v}$ is equal to 3 according to the nodes-covered-based interference model. With the above calculation method, link $\ell_{u,v}$ in Topo-II of Fig. 1 is also 3 in interference. But we note here that $\ell_{u,v}$ in Topo-I covers three links, $\ell_{u,a}$, $\ell_{u,c}$, and $\ell_{b,c}$ (excluding $\ell_{u,v}$ itself), while $\ell_{u,v}$ in Topo-II covers six links. In general, the more links there are in an area, the more traffics—which are to be scheduled by the routing protocols—will possibly flow through this area. As a result, Topo-II is more likely to experience local interferences around $\ell_{u,v}$ than Topo-I. To accurately weigh the interference of link, the number of covered links rather than the number of covered nodes should be taken into account.

Second, Topo-III of Fig. 1 shows another defect of the nodes-covered-based interference model. For Topo-III, no nodes are $|uv|$-covered by $\ell_{u,v}$, and then the interference of link $\ell_{u,v}$ is equal to zero. But, if node a has a link to u, then links $\ell_{u,v}$ and $\ell_{u,a}$ cannot be active (scheduled) at the same time. It is therefore unreasonable to say that $\ell_{u,v}$ in Topo-III, with the interference measure of zero, will not interfere with any other links.

Third, for Topo-I, it is sure to know $\ell_{u,v}$ interferes with $\ell_{u,a}$, $\ell_{u,c}$, and $\ell_{b,c}$, because all the end nodes of the later three links are $|uv|$-covered by u. Topo-IV of Fig. 1 shows another case in which node a has an incident link, $\ell_{a,x}$, but node x locates outside of the coverage of $\ell_{u,v}$. Recall that the two-way link model is used in this study; so $\ell_{u,v}$ exactly interferes with $\ell_{a,x}$, since there will be a potential conflict to a's ACK reception from x when u starts transmitting to v. Therefore, an effective link interference measure should also take into account the link who has only one end node that is covered.

In summary, the number of nodes covered by a link, even with realistic physical link model (for instance, the model proposed in Blough et al., 2007), is an ineffective indicator to measure the link interference. To cope with the defects of such a nodes-covered-based model, a new link interference model is proposed in this paper and its definition is as follows.

Definition 1. For a network graph $G(V,E)$, the interference of link $\ell_{u,v} \in E_G$, denoted by $I(\ell_{u,v})$, is equal to

$$|\{\ell_{x,y} | \ell_{x,y} \in E_G,\ x \text{ or } y \text{ or both is } |uv| - \text{covered by } u \text{ or } v\}|$$

Compared with the previous models, ours is also link-level interference model but it is based on the number of links actually interfered, instead of the number of nodes covered. For Topo-II and Topo-III in Fig. 1, the interferences of link $\ell_{u,v}$ are six and one, respectively, according to Definition 1, not three and zero, as calculated by the nodes-covered-based model. The proposed model is out of consideration that dynamic traffic flows are the essential reason leading to co-channel interferences; thus, a better idea of measuring the interference of a given link is to consider the number of links actually interfered with this given link. Our model intrinsically captures the link interference features caused by co-channel traffic flows and also, simulations show the efficacy of this idea in generating interference-aware topologies for wireless Ad hoc and sensor networks. The interference across the whole network, based on Definition 1, is defined in the following.

Definition 2. For a network graph $G(V,E)$, the interference of the network is defined as

$$I(G) = \max\{I_\ell, \ell \in E_G\}$$

We select the maximum link interference as the measure of the network interference, as Burkhart et al. (2004) and Moaveni-Nejad and Li (2005) do. The major reason behind is that as pointed out in the literature (Ramachandran et al., 2006; Wang et al., 2008; Gandham et al., 2008; Sun et al., 2013), the maximum link interference over a co-channel wireless network in Definition 2 determines the least number of time slots needed to schedule all links once without conflicts. So, for a network, minimizing the maximum link interference or deducing its lower bound is an appreciable way of achieving the throughput maximization or the latency minimization.

3.3. Algorithm for optimizing link interferences

Algorithm 1. Link interference optimization algorithm.

Require: $G(V_G, E_G)$, the communication graph
Ensure: $G'(V_{G'}, E_{G'})$, a sub-graph of G with minimum network interference

```
initialize G'(V_G', E_G') with V_G' = V_G and E_G' = ∅
for ∀ℓ ∈ E_G do
    update the interference weight of ℓ with I(ℓ) according to Definition Definition 1
end for
sort all links of E_G by the precedence metric defined in Eq. (1) such that for any two links ℓ_i and ℓ_j in E_G, that ω(ℓ_i) ≺ ω(ℓ_j) holds provided i < j
while E_G ≠ ∅ do
    choose link ℓ_{u,v} ∈ E_G such that its interference weight is the maximum
    while ‖p_{G'}(u,v)‖ > t × ‖uv‖ do
        find ℓ_{x,y} ∈ E_G with the minimum interference weight and insert it into E_G'
        delete ℓ_{x,y} from E_G
    end while
    delete ℓ_{u,v} from E_G if it has not yet been removed into E_G'
end while
```

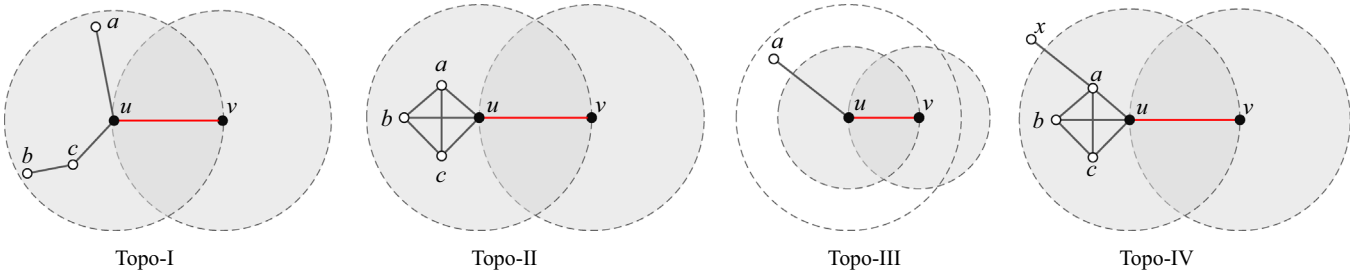

Fig. 1. Illustration of wireless co-channel link interference, in which it is assumed that link $\ell_{u,v}$ is active.

To comprehensively answer the performance of the proposed model and achieve interference-optimal topologies with both the energy spanner and the connectivity properties, this paper designs a centralized greedy algorithm (Algorithm 1) based on the proposed interference model. Before presenting our algorithm, we first introduce some necessary notations.

For a given network $G(V,E)$, let $p_G^*(u,v)$ and $\|p_G^*(u,v)\|$ represent the energy-minimum path between nodes u and v and the energy cost of this path, respectively, where $\|p_G^*(u,v)\|$ is the sum of the energy costs of all links along $p_G^*(u,v)$. If there is not any path between nodes u and v in G, then $\|p_G(u,v)\|=\infty$. If any pair of nodes u and v in G', a sub-graph of G, have an energy-minimum path with the energy cost of $\|p_{G'}(u,v)\|$ and $\|p_{G'}(u,v)\| \le t \times \|p_G^*(u,v)\|$ $(t>1)$, then G' is called a t-energy-spanner of G.

The first two primary steps of Algorithm 1 are to update the link interference for all the links, and to sort them by their link weights. Based on the interference model described in Definition 1, we here employ a precedence metric for comparing link weights. Let $\omega(\ell)$ denote the link weight of ℓ. For two distinct links $\ell_{u,v}$ and $\ell_{x,y}$, there is a precedence relationship between both of them, which is defined in Eq. (1). Note here that the link weight and the link interference are different: the former is a compound metric considering both the link interference and the link distance together

$$\omega(\ell_{u,v}) \prec \omega(\ell_{x,y}) \quad \text{if} \begin{cases} I(\ell_{u,v}) < I(\ell_{x,y}) & \text{or} \\ I(\ell_{u,v}) = I(\ell_{x,y}) & \text{but } |uv| < |xy| \end{cases} \tag{1}$$

Like the LISE algorithm (Burkhart et al., 2004), the proposed Algorithm 1 is also based on the greedy policy—it always struggles to replace the weight-maximum link of G by a t-energy spanner path that has already existed in G', and to insert the weight-minimum link of G into G'. Figure 2 shows the set of links sorted by Algorithm 1 (line 5), where $\ell_i \prec \ell_{i+1}$. At the final step of Algorithm 1, $(m-j+1)$ links $(\ell_m, \ell_{m-1}, \ldots, \ell_j)$ have been successively examined by the line-6 loop of Algorithm 1, while k links $(\ell_1, \ell_2, \ldots, \ell_k)$ have been inserted into $E_{G'}$. Note that in Fig. 2, k is possibly equal to j as Algorithm 1 terminates—in this case, link ℓ_j has to be inserted into $E_{G'}$ because no t-energy-spanner path connecting the two end nodes of ℓ_j can be found. In terms of the topology control performance, Algorithm 1 improves the LISE algorithm in two aspects.

First, Algorithm 1 (line 9) inserts links one by one, instead of inserting all possible interference-minimum links at a time, as LISE does. With doing so in Algorithm 1, link redundancy will be avoided in some extent—at least for the final iteration of line 6 in Algorithm 1.

Second, for obtaining an ordered set of links, Algorithm 1 (line 5) compares the link weights—which are determined by the precedence metric of Eq. (1)—rather than the link interferences, as LISE does. Intuitively, a distance-long link is generally easier to escalate interferences than the shorter one; and especially, the longer the distance of a link, the higher its energy cost. We analyze the impact of link distance on interferences in Fig. 3, in which for a given network, the link interferences are refreshed by LISE model

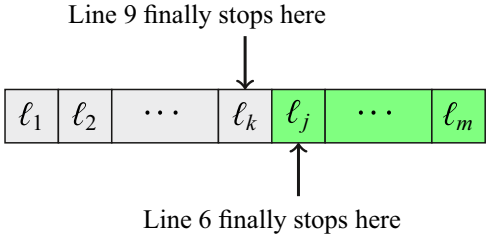

Fig. 2. Termination of Algorithm 1 on the set of sorted links of E_G. Upon Algorithm 1's termination, $k=j-1$ or $k=j$ and only links $\ell_i (1 \le i \le k)$ were inserted into $E_{G'}$.

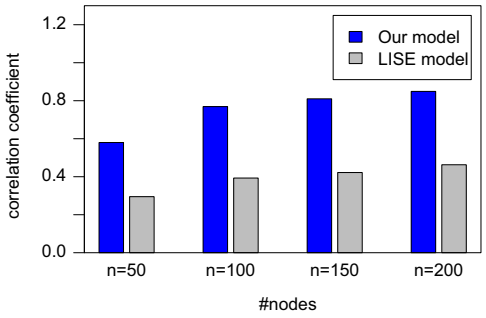

Fig. 3. The correlation between the link distance and its interference measured by two models, respectively. The stretch factor in all simulations is set to be five.

and our model, respectively, before topology control is performed on the network. Under our model, it can be seen that with the network scale increasing, the physical distance of a link strongly correlates to the interference brought by that link. But the correlation under the LISE model is not much significant. Indeed, under LISE, two links with identical interference are often rendered different link distances. Section 4 will demonstrate the improvement achieved by using our precedence metric to sort the links.

By three theorems, we next prove the properties of topologies achieved by Algorithm 1, including the connectivity, the t-energy spanner, and the optimality in interference.

Theorem 1. *If G is connected, the sub-graph G' constructed by Algorithm 1 is also connected.*

Proof. For any pair of nodes who have a link in G, after entering the loop of line 6 of Algorithm 1, it will be either replaced with a spanner path or directly inserted by line 9 of Algorithm 1. So, such two nodes are always connected even in G'. Now consider two nodes, say, u and v who have no link to each other in G. In that G is connected, suppose there exists a path between u and v in G, which is consisted of a set of links, $\ell_{u,x_1}, \ell_{x_1,x_2}, \ldots, \ell_{x_k,v} (k \ge 1)$. According to the above analysis, each of the links along the path between u and v in G will be connected in G'. Thus, u and v are sure to be connected in G' □

Theorem 2. *The sub-graph G' constructed by Algorithm 1 is a t-energy-spanner of graph G $(t>1)$.*

Proof. Since $V_G = V_{G'}$ and G' is connected according to Theorem 1, we know that for any given two nodes, u and v, there are at least one paths connecting both of them in G'. Figure 2 shows the general status when Algorithm 1 terminates, where $m=|E_G|$ and $1 \le k \le j \le m$. As for links that are in E_G but are not included in $E_{G'}$, i.e., the links in $\{\ell_j, \ldots, \ell_m\}$ shown in Fig. 2, Algorithm 1 will have replaced them with t-energy-spanner paths that can connect their end nodes—of course, these spanner paths are established by inserting appropriate links into $E_{G'}$ continuously. Thus, two nodes who have a link in $\{\ell_j, \ldots, \ell_m\}$ must have a t-energy-spanner path that connects both of them.

Upon Algorithm 1's termination, k links have been inserted into $E_{G'}$ according to Fig. 2; and all the k links construct $(m-k+1)$ t-energy-spanner paths which entirely cover all the nodes of G because we have $V_{G'} = V_G$. It is thus obvious that for any pair of nodes in G, there is always either a link or a path to connect both of them in G'. Furthermore, according to the Bellman optimality, we know that the sub-path of a t-energy-spanner path is still of t-energy-spanner as well. So, the above analysis is sufficient to prove

the existence of t-energy-spanner path in G' for any pair of nodes in G. □

It is less straightforward to prove that Algorithm 1 can achieve the interference-optimal topology, we first introduce the concept of conflict graph (Ramachandran et al., 2006; Gandham et al., 2008; Sun et al., 2013). As shown in Fig. 4, conflict graph G_{conf} is constructed from original graph G: in detail, G_{conf}'s vertices are converted from the edges of G, and if two edges (links) of G interfere with each other, then there is an edge in G_{conf}. For instance, edge $\ell_{b,c}$ interferes with edge $\ell_{a,b}$ in G, and then there exists an edge between vertices (b,c) and (a,b) in G_{conf}. In addition, even though $\ell_{b,c}$ and $\ell_{e,f}$ are not incident in G, both of them do still interfere with each other; so in G_{conf}, there is an edge connecting vertices (b,c) and (e,f). It is clear that for a graph of co-channel wireless network, its conflict graph—actually the greatest vertex degree of the conflict graph—can appreciably profile the interferences of original graph.

Theorem 3. *The sub-graph G' constructed by Algorithm 1 is interference-optimal.*

Proof. Recall that for a given network graph G, the network interference, $I(G)$, is defined as the maximum link interference among all links. According to the function of conflict graph mentioned in the above, the procedure of Algorithm 1 essentially is that of iteratively choosing vertices of the conflict graph of G. For each iteration, Algorithm 1 always chooses the vertex with the least degree in conflict graph G_{conf}. When Algorithm 1 terminates, therefore, the finally chosen vertex (a link in G) of G_{conf} is sure to have the least degree, which will determine the minimum $I(G)$. □

3.4. Discussions

Unlike the node-covered-based models, the proposed link interference model measures the interference of link $\ell_{u,v}$ by counting the number of links who have at least one end nodes $|uv|$-covered by (interfered with) $\ell_{u,v}$. Our model will work with only the knowledge of the neighborhood information—without knowing the node location and the radio coverage characteristics *in priori*, and without assuming the range-homogeneous radios. In practice, the link neighborhood can be achieved only by local message exchanging, regardless of what metrics to be used to determine the existence of a link (e.g., by the physical link distance, the RSSI, the PRR, or other metrics). So our model can also be easily calculated in a distributed manner. In addition, our model takes into account the two-way link communication, which is more realistic than traditional UDG models. In Burkhart et al. (2004), a distributed algorithm is proposed to achieve a near-optimal topology based on their interference model. Traditional interference-reducing approaches did not fully consider the realistic cases as depicted in Fig. 1, and consequently, they might still suffer significant interference, even though they prove correct and efficient on the algorithmic level. Actually, combined with our model, all the previous algorithms that aim to reduce network interference could accomplish better topology control almost without the least modification. This paper is mainly concerned about a model for effectively profiling link interference in topology control; constructing interference-optimal topology based on our model in a distributed way is out of the scope of this paper and it will be our future work.

Our centralized algorithm inserts links one by one into the constructed topology, rather than simultaneously inserting all the interference-minimum links as LISE does, so more computations in form of loops might be required. But, this way compensates for the deficiency with quite less links left in the constructed topologies. Moreover, simulation results show that even with much sparser topologies output, our designs can achieve energy-minimum paths that are indistinctively higher than LISE in terms of average energy cost.

It is noticeable that LISE is to construct distance-spanner topologies, instead of energy-spanner ones. The difference between these two spanner properties is nontrivial in optimization; and simulations imply that LISE cannot effectively construct energy-spanner interference-aware topologies—leaving too many links in the constructed topologies. The reason behind is as follows. Figure 5 shows five links. Here suppose that the energy cost of each link is equal to the square of its physical link distance, and that a t-spanner path is to be found. For link $\ell_{u,v}$ in Fig. 5, path $\{\ell_{u,b} \rightarrow \ell_{b,a} \rightarrow \ell_{a,c} \rightarrow \ell_{c,v}\}$ is a t-distance-spanner path connecting u and v, if t is set to be not less than $\sqrt{2}$, otherwise, only link $\ell_{u,v}$ itself is the t-distance-spanner path to be found. If we want to find a t-energy-spanner path for u and v with $t \geq 1$, however, the above path is 8 in total energy cost, far less than the energy cost of $\ell_{u,v}$ which equals 16. It seems that the energy-spanner path is easier to be established than the distance-spanner one, especially in the case with strict stretch factors or dense network deployment.

But the problem facing the energy-spanner path establishment is that more links may be involved in the satisfactory paths of energy spanner. Though our algorithm and LISE both employ greedy policy, LISE involves more links in the final topology and these links are often rendered longer distance, as shown in Fig. 6. These two features reflected in LISE are, however, unfavorable to reduce network interference. Such a difference in topology control performance is essentially caused by the difference of two interference models in use. Measuring the number of links $|uv|$-covered by link $\ell_{u,v}$ as $\ell_{u,v}$'s interference can itself imply the

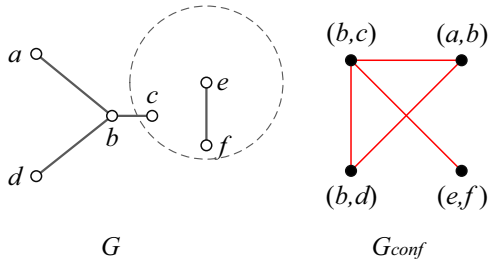

Fig. 4. Conflict graph G_{conf} constructed from G. In G, node c locates within the coverage of $\ell_{e,f}$ and then $\ell_{e,f}$ interferes with $\ell_{b,c}$.

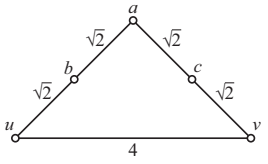

Fig. 5. Illustration of spanner path determination where the numbers associating with links represent the physical link distance.

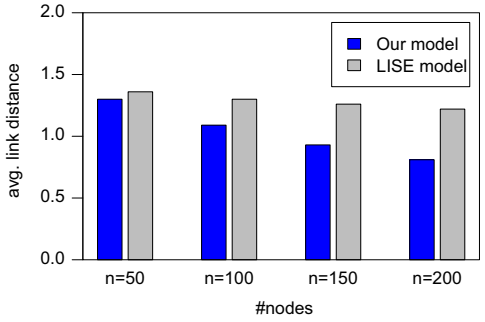

Fig. 6. Comparison of the average distances of links in topologies constructed by two algorithms, respectively. In all simulations the stretch factor and the maximum radio range of all nodes are set to be five and two, respectively.

information of link distances, because the physical distance of two nodes determines whether there exists a link between both of them. Combining Figs. 3 and 6, we can conclude that considering links' physical distances benefits the efficacy of the link interference model. More other detailed analysis of the advantages of our model will be provided later in Section 4.

4. Evaluation

We use C++ to program a link-level topology simulator, on which we conduct a series of experiments, in order to evaluate our designs.

4.1. Experimental settings and metrics

In simulations all nodes are randomly deployed in a uniform manner within a 20×20 square. The maximum radio range is set to be 2 for all nodes. Each point is reported with the average of 100 repetitions with random seeds. We focus on constructing interference-aware topologies with the energy spanner rather than the distance spanner. Additionally, in all simulations we consider a many-to-one and energy-efficient routing scenario, in which a sink node locates at the left-bottom corner of the network area and others nodes, randomly deployed in the network area, use t-energy spanner paths to deliver their data to the sink node. Such a many-to-one communication is widely adopted by wireless sensor network applications gathering physical signals. In each simulation, after all the nodes are deployed, we use the UDG model to establish an original network graph, on which the LISE algorithm and our algorithm run respectively. It is worthy to note that even though the disk radio coverage is assumed in simulations, the neighborhood information is the only requirement for our model and algorithm. We employ three metrics to evaluate our designs by comparing with LISE:

- *%Links*: the ratio of $|E_{G'}|/|E_G|$, after performing topology controls on the original network graph G.
- *Ceep*: the average cost of energy-minimum paths in the constructed topology G'.
- *MaxIntf*: the maximum vertex degree of the conflict graph converted from the constructed topology G'.

It is easy to understand the function of the first metric—the less the number of links in the resulted graph, the less the network interference may be. The second metric weighs the energy efficiency of the topology control in use. We have introduced the function of conflict graph. Taking it a further step, we know, according to the graph coloring principles, that the greater the maximum degree of a conflict graph, the longer the time that we need to schedule all links once without co-channel conflicts. Therefore, the maximum degree of conflict graph, served as the third metric, can reasonably indicate the network performances in terms of throughput and latency.

The remainder of this section first shows a few topologies resulted by our algorithm and LISE for visual comparisons. Second, the proposed precedence metric for sorting link weights is examined just on LISE's operation. Finally, more detailed comparisons of our model and LISE model are given in terms of metrics *%Links*, *Ceep*, and *MaxIntf* defined in the above.

4.2. Results and analysis

4.2.1. Comparisons of the overall topologies

Figures 7 and 8 show a few simulation graphs which visualize the comparisons between our interference model and the LISE model. From both figures we can see a sharp contrast: the topologies derived by our model have obviously less links than that by the LISE model, especially when the network scale becomes larger. Additionally, one remarkable difference is that the topologies of LISE have dense links nearby the boundary of the network area. Simulations with other configurations present similar results as well. The LISE model measures the link interference only according to the number of nodes the link can cover, while the links close to boundary are sure to cover less nodes than links inside of the network area does. So, such boundary-near links are often chosen preferably in LISE's topology construction. In general, the less the links a network involves, the lower the degree that the network experiences interferences. Quantitative comparisons will be given in later sections. Next we statistically compare two interference models.

In Figs. 9 and 10, we compare the distributions of link interference under LISE model and our model with 100 and 200 nodes, respectively. To measure the interference of a link, LISE model considers only the number of nodes this link covers, while our model counts the number of links actually interfered with this link. As a result, the link interferences calculated by LISE model distribute in a smaller range. For instance, in the simulation with 100 nodes, the link interference of LISE ranges roughly from 0 to 25, while that of our model ranges from 0 to 200. In fact, the range of link interferences is of little use for accounting for the topology control performance; but, their distribution and density characteristics make more sense.

It is observed in Figs. 9 and 10 that for LISE model, the link interferences are relatively distinguishable (clustering) in the distribution density and rug plots, i.e., there are many links that are rendered identical interference. In consequence, LISE will simultaneously insert interference-identical links into the constructed graph in each iteration—going an aggressive step—without considering whether all the inserted links are helpful to construct connected network with

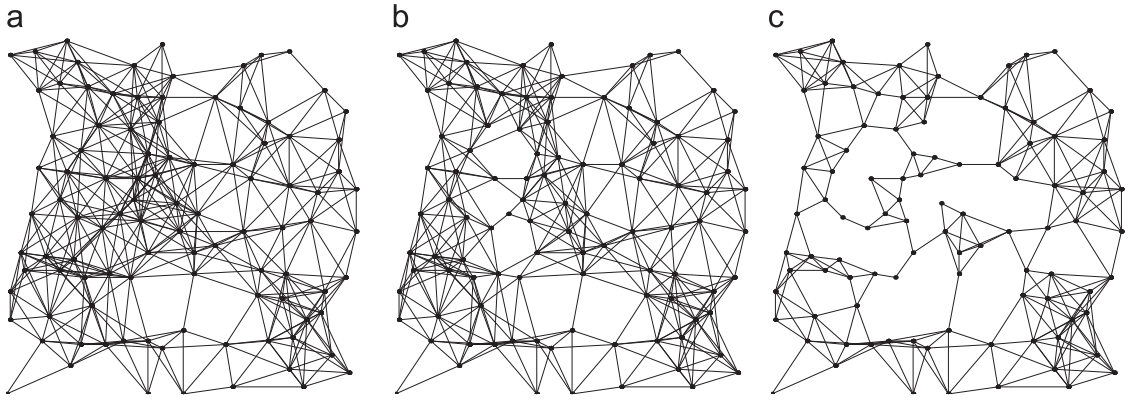

Fig. 7. Comparison of original graph and resulted topologies (the number of nodes and the stretch factor are set to be 100 and 5, respectively): (a) original graph, (b) by LISE model, and (c) by our model.

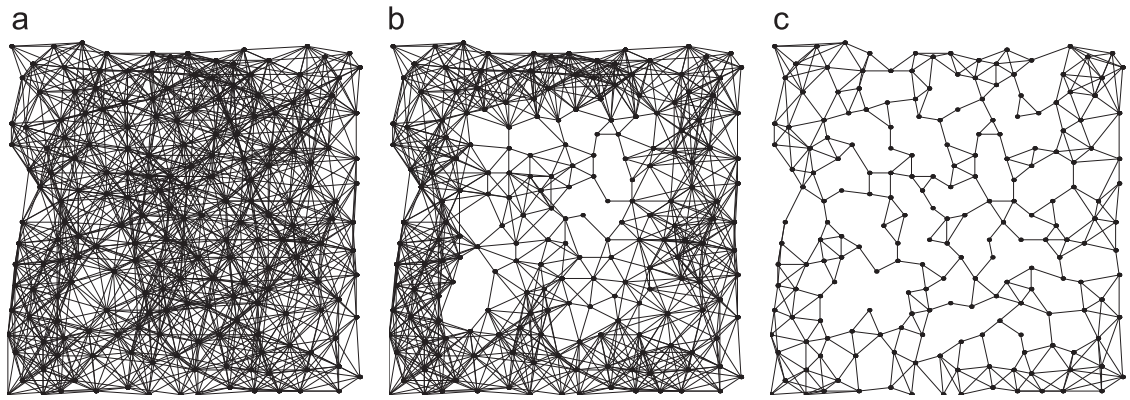

Fig. 8. Comparison of original graph and resulted topologies (the number of nodes and the stretch factor are set to be 200 and 5, respectively): (a) original graph, (b) by LISE model, and (c) by our model.

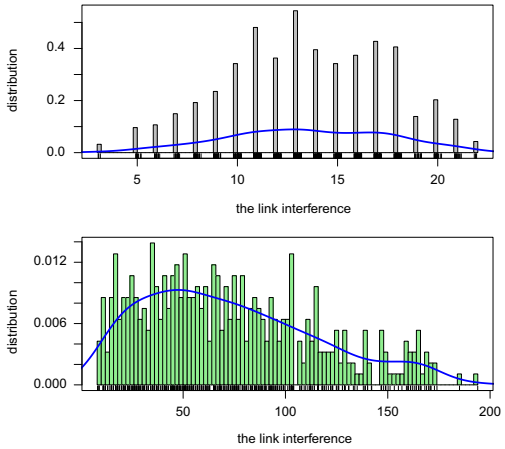

Fig. 9. Distributions of link interferences calculated by two models (top: LISE model, bottom: our model). The number of nodes and the stretch factor are set to be 100 and 5, respectively.

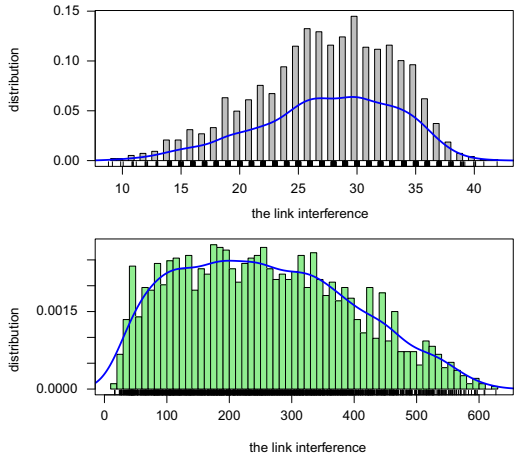

Fig. 10. Distributions of link interferences calculated by two models (top: LISE model, bottom: our model). The number of nodes and the stretch factor are set to be 200 and 5, respectively.

spanner paths. For our model, however, the link interferences are rather uniform, which makes our algorithm go forward with a prudent step—at a time, inserting the most indispensable links into the target graph. That is also the essential reason that our algorithm achieves so less links as shown in Figs. 7 and 8. In all simulations, the distributions of link interferences under two models behave like what

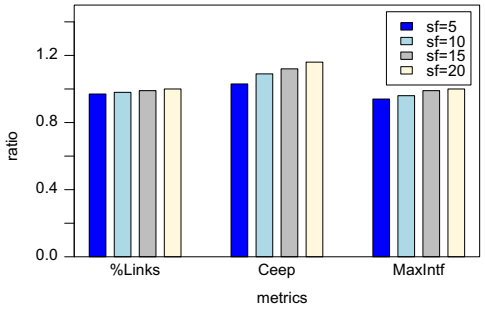

Fig. 11. Comparison of performances of LISE with and without using the precedence metric. The notation of stretch factor is abbreviated as "sf" and the number of nodes are all set to be 100 for all simulations here.

Figs. 9 and 10 plot; due to the page limit we present only these two figures.

4.2.2. *The precedence metric for sorting link weights*

For LISE, it always inserts all the interference-minimum links into the resulted graph at a time; with doing so, redundant links or distance-longer links close to boundary might be chosen with high probability, as analyzed in Section 3.4. To deal with this problem, we first propose a precedence metric in Eq. (1) that takes into account the physical link distance, aimed at discriminating links with identical interference, and then we construct the interference-aware topology by inserting links one by one in Algorithm 1. To effectively demonstrate the function of the proposed precedence metric, we examine it only in LISE's simulations. Figure 11 plots the performance of LISE with and without using our precedence metric in sorting links. It can be seen that with the precedence metric adopted by LISE, both the number of links and the maximum interference in the derived topology decrease, while the average energy cost of energy-minimum paths does not increases substantially with the ratios less than 1.2. With the stretch factor increasing, the performance improvements both in terms of *%Links* and *MaxIntf* tend to be indistinctive because the larger stretch factor will retain as small fraction of links as possible in the resulted topologies, which confines both the establishment of more energy-efficient paths and the interferences caused by close-by links. Figure 12 further illustrates the advantage of the precedence metric for LISE. With smaller stretch factors in simulations, like 5 and 10, the number of links in the constructed topologies reduces by 10%, which in turn reduces the maximum network interference by 12–20%.

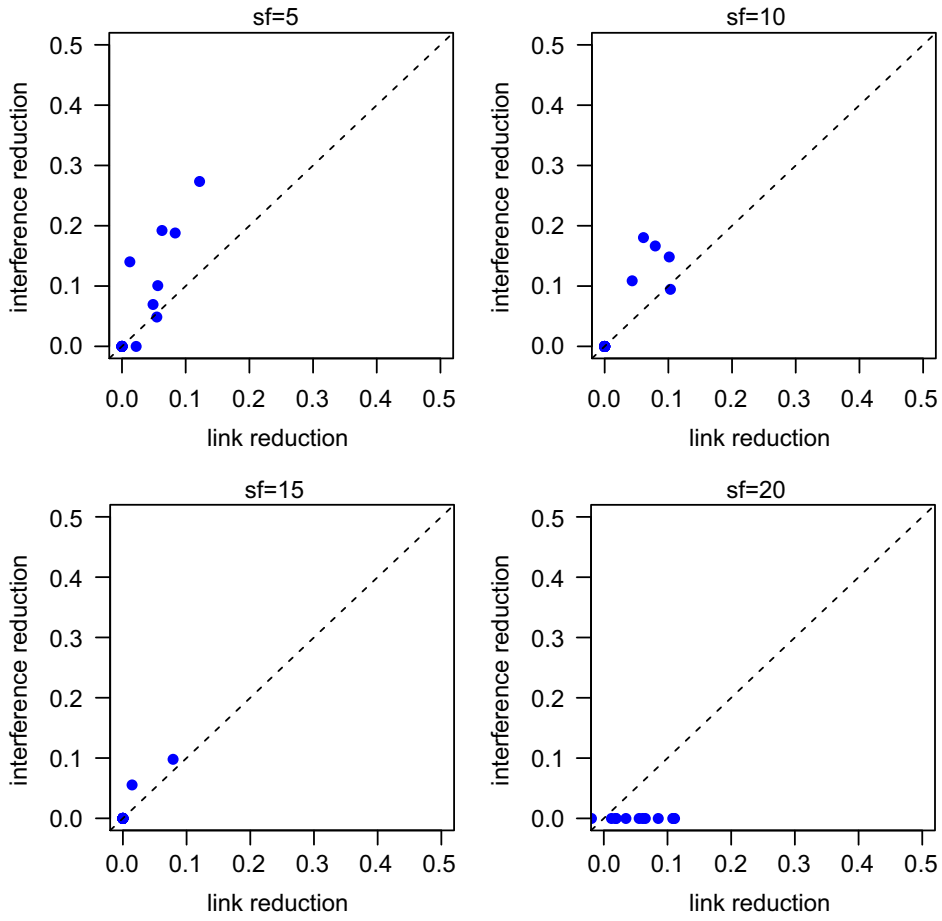

Fig. 12. Correlation of the link number reduction and the link interference reduction in LISE with and without using the precedence metric. The notation of stretch factor is abbreviated as "sf" and the number of nodes are all set to be 100 for all simulations here.

4.2.3. Comparisons by %Links, Ceep and MaxIntf

This section shows the performance improvement of our model in terms of three metrics defined in the above. Figure 13 plots the performance of LISE and our designs in terms of *%Links*, i.e., the ratio between the number of links left in final topologies and the number of links in original network graphs. Given a stretch factor, our algorithm always achieves lower *%Links*. In particular, with the network scale increasing, the fractions of left links under two models both fall. But the link reduction under our algorithm is more aggressive than that under LISE; such an improvement exists thanks to the inherent distribution characteristics resulted from our interference model. It is worthy to note that for topology controls targeting robustness, more redundant links may be required but the ensuing interference increment is not the major consideration. Determining a robustness-constrained link interference optimization is out of the scope of this study. In our extensive repetitive experiments, however, we find that for most topologies constructed by our designs, the node degree is at least two and will tend to increase as the network scale increases—which empirically reflects the possible robustness the proposed algorithm can achieve.

Figure 14 shows the energy spanner performance. Since less links are inserted into the constructed topologies, the average energy cost of energy-minimum paths is higher with our designs—the ratios of our *Ceep* and LISE's *Ceep* are always beyond 100% but never greater than 1.2. When the network scales are relatively less, say, 50, our model is a little better than LISE in terms of *%Links* as shown in Fig. 13 and consequently, the ratios of our *Ceep* and LISE's *Ceep* almost always reach to one in Fig. 14. As the network scale increases up to 100 or greater, the number of links left in the final topologies by our designs falls more quickly than LISE—our algorithm involves only 20–55% links of original network. Nevertheless, such significant link reductions moderately impact the average energy cost of spanner paths such that the ratios of our *Ceep* and LISE's *Ceep* are kept to at most 1.2 in simulations.

As for the interference-controlling performance, our design overwhelms LISE with remarkably low network interference, especially as the network scale increases. For instance, in Fig. 14, the ratios of our *MaxIntf* and LISE's *MaxIntf* are only 40–50% and 20–25% when the numbers of nodes are set to be 100 and 200, respectively. As described in the above, our algorithm outputs topologies with significantly less links, which can in turn reduce the *MaxIntf* of those topologies.

5. Conclusions and future work

This study has proposed a new model for measuring the link interference in wireless Ad hoc and sensor networks. Different than the previous node-covered-based model, our model measures the interference of a link by counting the number of links that are covered (interfered with) the given link. Additionally we have also presented a centralized algorithm to achieve interference-optimal topologies and then to evaluate our model. In particular, unlike early attempts, the proposed algorithm takes into account the impact of link distance on the topology construction, thereby further improving the performance of topology control. Extensive simulations with diverse configurations were conducted in this paper, and the simulation results demonstrate the efficacy of our model and algorithm—dramatic reduction of links

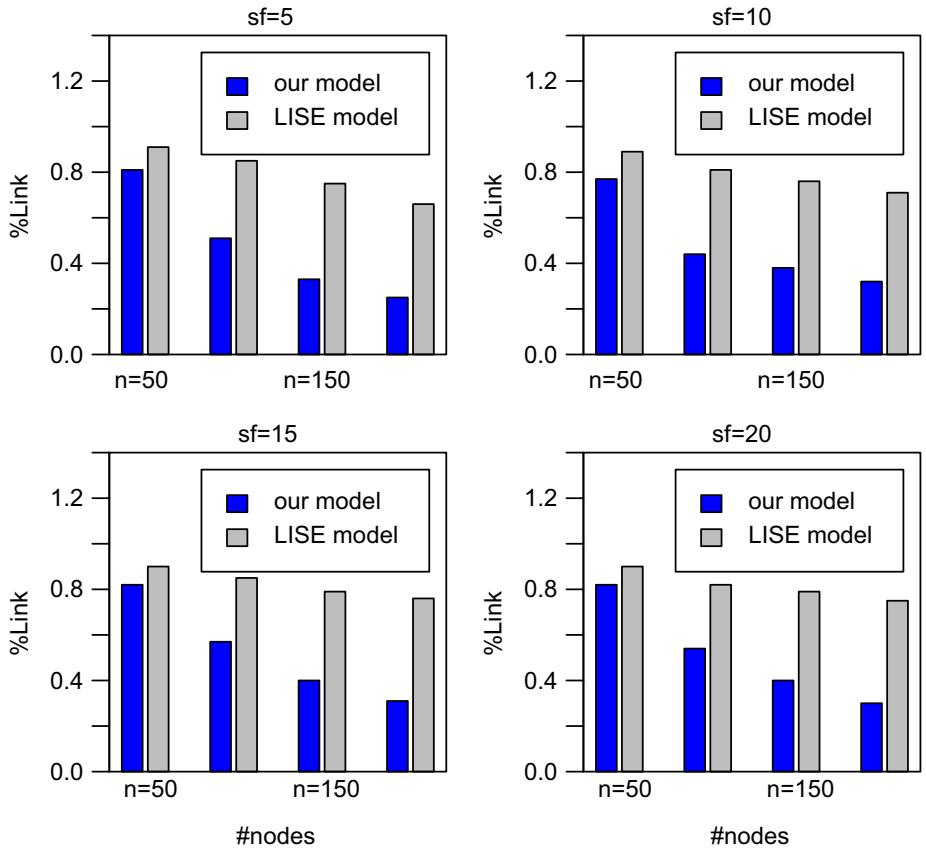

Fig. 13. Comparison of the number of links in the constructed graphs. The notation of stretch factor is abbreviated as "sf".

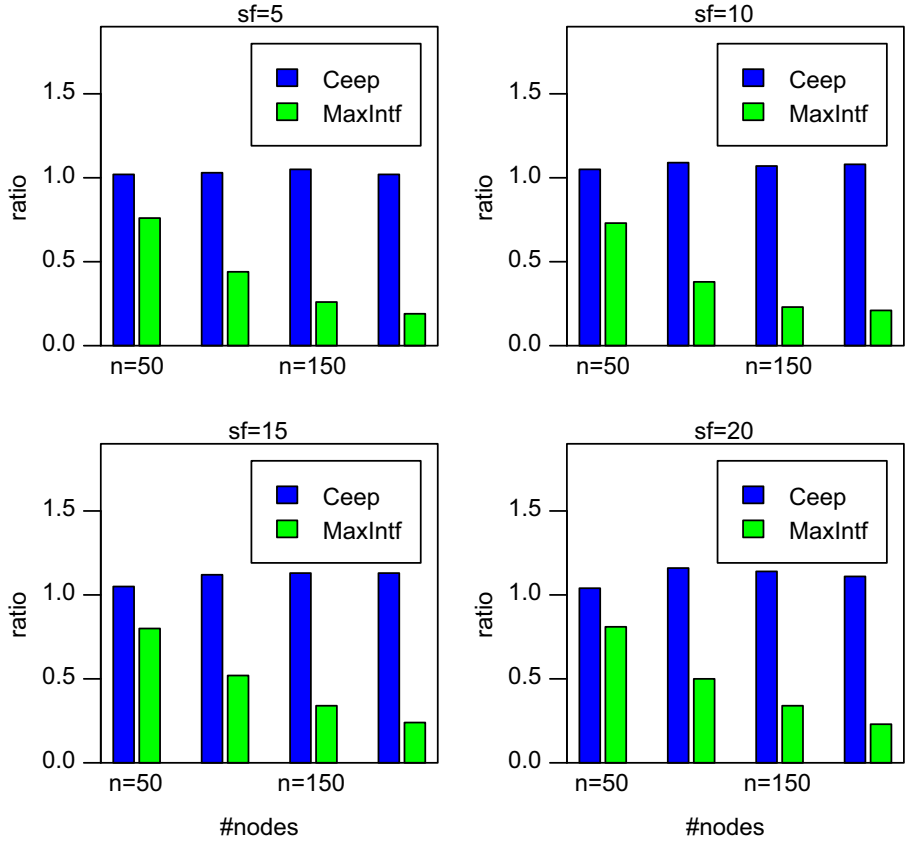

Fig. 14. Comparison of *%Ceep* and *MaxIntf* under two models where each bar plots the ratio of our model to LISE model. The notation of stretch factor is abbreviated as "sf".

and then significantly low network interferences can be achieved in final topologies, all without degrading the performance of energy spanner. Meanwhile, we found that the previous models based on the number of covered nodes are neither suitable to construct interference-aware topologies of energy spanner, nor effective to discriminate links that are near by the network boundary but have longer physical distance. The proposed model is independent of the topology control algorithms in use, so it can be directly fed into previous topology control algorithms aimed at minimizing global link interference. In the future we will focus largely on designing efficient distributed algorithms to construct interference-optimal topologies based on our model.

Acknowledgments

The first three authors were supported by the NSF of China with Grant no. 61300180 and partially by the Fundamental Research Funds for the Central Universities of China with Grant no. TD2014-01. The fourth author was supported, in part, by the NSF of China with Grant no. 51378156 and the Ministry of Science and Technology Project with Grant no. 2011BAK02B01.

References

Ababneh N. Performance evaluation of a topology control algorithm for wireless sensor networks. Int J Distrib Sensor Netw 2010;2010:1–16. http://dx.doi.org/10.1155/2010/671385.

Aziz A, Sekercioglu YA, Fitzpatrick P, Ivanovich M. A survey on distributed topology control techniques for extending the lifetime of battery powered wireless sensor networks. IEEE Commun Surv Tutor 2013;15(1):121–44.

Blough D, Leoncini M, Resta G, Santi P. Topology control with better radio models: implications for energy and multi-hop interference. Perform Eval 2007;64:379–98.

Burkhart M, Rickenbach P, Wattenhofer R, Zollinger A. Does topology control reduce interference. In: MobiHoc, Roppongi, Japan; 2004. p. 9–19.

Chiwewe T, Hancke G. A distributed topology control technique for low interference and energy efficiency in wireless sensor networks. IEEE Trans Ind Inf 2012;8(1):11–20.

Chong C, Kumar S. Sensor networks: evolution, opportunities, and challenges. In: Proceedings of IEEE, vol. 91; 2003. p. 1247–56.

Enam R, Qureshi R, Misbahuddin S. A uniform clustering mechanism for wireless sensor networks. Int J Distrib Sensor Netw 2014;2014:1–14.

Gandham S, Dawande M, Prakash R. Link scheduling in wireless sensor networks: distributed edge-coloring revisited. J Parallel Distrib Comput 2008;68:1122–34.

Hermans F, Rensfelt O, Voigt T, Ngai E, Norden L, GP. Sonic: classifying interference in 802.15.4 sensor networks. In: IPSN; 2013. p. 55–66.

Huang J, Liu S, Xing G, Zhang H, Wang J, Huang L. Accuracy-aware interference modeling and measurement in wireless sensor networks. In: ICDCS; 2011.

Jain K, Padhye J, Padmanabhan V, Qiu L. Impact of interference on multi-hop wireless network performance. In: MobiCom. 2003; p. 66–80.

Johanasson T, Carr-Motyckova L. Reducing interference in ad hoc networks through topology control. In: DIALM-POMC, Cologne, Germany; 2005. p. 17–23.

Lee C-Y, Yang C-S. Distributed energy-efficient topology control algorithm in home m2m networks. Int J Distrib Sensor Netw 2012;2012:1–8. http://dx.doi.org/10.1155/2012/387192.

Liu S, Xing G, Zhang H, Wang J, Huang J, Sha M, Huang L. Passive interference measurement in wireless sensor networks. In: ICNP. 2010. p. 52–61.

Liu L, Wang R, Xiao F. Topology control algorithm for underwater wireless sensor networks using gps-free mobile sensor nodes. J Netw Comput Appl 2012;35(6):1953–63.

Macedo M, Grilo A, Nunes M. Distributed latency-energy minimization and interference avoidance in tdma wireless sensor networks. Comput Netw 2009;53(5):569–82.

Moaveni-Nejad K, Li X. Low-interference topology control for wireless ad hoc networks. Ad Hoc Sensor Wireless Netw 2005;9(53):41–64.

Moscibroda T, Wattenhofer R, Zollinger A. Topology control meets sinr: the scheduling complexity of arbitrary topologies. In: MobiHoc, Florence, Italy; 2006. p. 310–21.

Ramachandran K, Belding E, Almeroth K, Buddhikot M. Interference-aware channel assignment in multi-radio wireless mesh networks. In: INFOCOM; 2006. p. 1–12.

Rickenbach P, Schmid S, Wattenhofer R, Zollinger A. A robust interference model for wireless ad-hoc networks. In: IPDPS; 2005. p. 239–46.

Rickenbach P, Wattenhofer R, Zollinger A. Algorithmic models of interference in wireless ad hoc and sensor networks. IEEE/ACM Trans Netw 2009;17(1):172–85.

Schmid S, Wattenhofer R. Algorithmic models for sensor networks. In: IPDPS; 2006. p. 1–11.

Sun G, Qiao G, Zhao L. Efficient link scheduling for rechargeable wireless ad-hoc and sensor networks. EURASIP J Wireless Commun Netw 2013;2013(223):1–14.

Wang Y, Wang W, Li X, Song W. Interference-aware joint routing and tdma link scheduling for static wireless networks. IEEE Trans Parallel Distrib Syst 2008;19(12):1709–25.

Yick J, Mukherjee B, Ghosal D. Wireless sensor network survey. Comput Netw 2008;52:2292–330.